Mol Cell Toxicol (2017) 13:305-315
DOI 10.1007/s13273-017-0034-5

ORIGINAL PAPER

6-Hydroxydopamine induces nuclear translocation of apoptosis inducing factor in nigral dopaminergic neurons in rat

Hong-Il Yoo[1], Gil-Yeong Ahn[1,2], Eun-Jin Lee[1], Eu-gene Kim[1], Sung-Young Hong[1], Sang-Jin Park[1], Ran-Sook Woo[1], Tai-Kyoung Baik[1] & Dae-Yong Song[1]

Received: 27 July 2016 / Accepted: 30 August 2016

Abstract Parkinson's disease (PD) is a progressive neurodegenerative disorder, characterized by relatively selective death of dopaminergic (DA) neurons in the substantia nigra pars compacta (SNpc). 6-Hydroxydopamine (6-OHDA), a neurotoxin that causes the death of DA neurons, is commonly used to produce experimental PD model in rodents. Accumulating evidences suggest that caspase-independent apoptotic programmed cell death (PCD) could also be involved in the progression of various neurodegenerative diseases in addition to caspase-dependent neuronal PCD. Apoptosis-inducing factor (AIF), a mitochondrial intermembrane oxidoreductase, has been identified as a key protein implicated in caspase-independent apoptosis. However, little is known about the role of AIF in death of nigral DA neurons in PD. Therefore, we undertook this study in an effort to clarify the involvement of AIF in DA neuronal death by 6-OHDA administration. Ten and twenty micrograms of 6-OHDA was infused into the medial forebrain bundle (MFB) unilaterally, and the experimental rats were sacrificed at various time point. The DA neuronal loss was identified in the ipsilateral SN in the dose-dependent manner by using NeuN and tyrosine hydroxylase immunohistochemical staining and western blot assay. Numerous degenerating neurons, showing apoptotic features which are characterized by the shrunken nuclei with eosinophilic perikarya were observed in the ipsilateral SNpc. Activating transcription factor 3 (ATF3), the specific marker for neuronal damage, was expressed in the ipsilateral DA neurons only. Immunohistochemistry and immunofluorescence staining demonstrated that nuclear localization of AIF in the ipsilateral degenerating DA neurons. These results suggest that AIF could induce DA neuronal death by caspase-independent apoptosis in 6-OHDA treated model, although other cell death cascades should not be rule out.

Keywords: Apoptosis inducing factor (AIF), Parkinson's disease, Activating transcription factor 3 (ATF3), 6-Hydroxydopamine (6-OHDA), Caspase-independent apoptosis

Introduction

Parkinson's disease (PD) is a common neurodegenerative disorder characterized by the formation of eosinophilic intraneuronal inclusions, called Lewy bodies, and gradual loss of dopaminergic (DA) neurons in the substantia nigra pars compacta (SNpc). These DA neurons form neural circuits with the striatum, subthalamic nuclei, thalamus, and neocortex, which act in concert to modulate voluntary motor movement. This neural circuit explains the clinical motor impairments in PD, such as resting tremor, muscle rigidity, postural instability, akinesia, and bradykinesia[1]. Although the precise etiology of PD remains unknown, oxidative stress, impaired energy production, and aberrant protein degradation have been implicated in the pathology. Neurotoxins, such as 1-methyl-4-phenyl-1,2,3,6-tetrahydropyridine (MPTP) and 6-hydroxy dopamine (6-OHDA) mimic many of these hallmark characteristics of PD and have been widely used to generate animal models of this disorder[2,3].

6-OHDA is a hydroxylated analogue of dopamine

[1]Department of Anatomy and Neuroscience, School of Medicine, Eulji University, Daejeon, Republic of Korea
[2]Department of Orthopaedic Surgery, Pohang St. Mary's Hospital, Pohang, Republic of Korea
Correspondence and requests for materials should be addressed to T.-K. Baik (✉jbl0719@naver.com) & D.-Y. Song (✉dysong@eulji.ac.kr)

that induces selective cell death of catecholaminergic neurons in the central nervous system. 6-OHDA toxicity is thought to be mediated by selective uptake through the DA transporter. Under physiological conditions, the absorbed 6-OHDA is auto-oxidized and then induce nigrostriatal dopaminergic lesions via generation of reactive oxygen species (ROS)[4-6].

Several *in vitro* studies have suggested that 6-OHDA may induce DA neuronal cell death through a caspase-dependent apoptosis mechanism[7,8]. However, both overexpression of the anti-apoptotic protein Bcl-2 and inhibition of caspase activation by the caspase inhibitors, zVAD-FMK or Ac-DEVD-CHO, are insufficient to completely block DA neuronal death after 6-OHDA exposure[9]. Ebert and colleagues also demonstrated *in vivo* evidences that injection of 6-OHDA into adult rat striatum did not activate caspase-9 or caspase-3 or increase levels of caspase-dependent cleavage products in the SNpc at various time points, even though DA neuronal cell loss was ongoing[10]. These reports support that other cell death pathways may be involved in 6-OHDA-mediated neurotoxicity to DA neurons.

Apoptosis-inducing factor (AIF) is a phylogenetically conserved mitochondrial flavoprotein encoded by a 16 exon-containing gene located on chromosome X, region q25-26, and A6 in humans and mice, respectively[11]. AIF is normally anchored in the outer mitochondrial membrane and has been proposed to act as a putative ROS scavenger[12]. However, under some pathological conditions, the anchored mature AIF (67 kDa) is further processed to a ~57 kDa form by activated calpains and/or cathepsins[13]. This soluble pro-apoptotic AIF form, called truncated AIF (tAIF) is translocated into the nucleus via its C-terminal domain nuclear localization sequence, which leads to large-scale DNA fragmentation and apoptosis[13,14]. A majority of studies have reported that release of AIF does not require caspase activation[15,16], and these characteristics of AIF have lead researchers to recognize AIF as a molecule that can induce caspase-independent apoptosis.

Based on the previous studies that DA neuronal cell death triggered by 6-OHDA could be caused by the caspase-independent apoptosis pathway and AIF induces caspase-independent apoptosis, we hypothesized that AIF may involve a DA neuronal death after 6-OHDA exposure. Therefore, in the present study, we have examined the expression pattern and nuclear translocation of AIF following 6-OHDA treatment.

Results

6-OHDA induces gradual loss of DA neurons in a dose-dependent manner

Compared with the contralateral SN, a dose-dependent decrease in the number of TH-immunoreactive (ir) cell bodies was detected in the ipsilateral SN (Figure 1A). The number of TH-ir cell bodies and the density of TH-ir fibers decreased in a dose-dependent manner. To confirm whether the reduction in TH immunoreactivity in the ipsilateral SN was caused by loss of DA neurons or by blockage of DA biosynthesis due to 6-OHDA toxicity, immunohistochemistry with anti-NeuN was performed. Consistent with the TH-immunohistochemistry results, the number of NeuN-ir neurons in the ipsilateral SNpc decreased following 6-OHDA exposure (Figure 1B). However, the intensity and number of NeuN-ir neurons in other midbrain regions, such as the red nucleus and substantia nigra pars reticulata (SNpr), did not change. These results show that the unilateral 6-OHDA lesion in medial forebrain bundle induced specific ipsilateral DA neuronal degeneration. A western blot assay was performed to determine the cell death ratio in accordance with the amount of 6-OHDA used. The amount of TH protein in the ipsilateral SN compared to that in the contralateral SN was 62.4 ± 9.7% (mean ± standard deviation) and 25.1 ± 12.9% following 10 μg and 20 μg of 6-OHDA administration into the MFB at 7 days post-lesion (dpl) (Figure 1C and D).

ATF3 induction precedes 6-OHDA-induced DA neuronal apoptotic cell death

A previous study from our laboratory showed that transecting the rat MFB induces gradual apoptotic degeneration of DA neurons in the ipsilateral SNpc, and this apoptotic cascade is initiated by induction of ATF3 and c-Jun phosphorylation[17]. Therefore, we performed ATF3 immunohistochemistry and H & E staining to investigate the type of DA neuronal cell death. Following 6-OHDA treatment into the MFB, specific ATF3 expression was detected in the ipsilateral SNpc (Figure 2A). No ATF3-ir nuclei were found in the contralateral SNpc. To examine whether 6-OHDA-treated DA neurons specifically expressed ATF3, double immunofluorescence with anti-ATF3/TH was performed. All ATF3-ir nuclei were exactly co-localized with the TH-ir neurons in the ipsilateral SNpc (Figure 2B). To trace the expression level of ATF3 in accordance with the amount of the 6-OHDA, the western blot assay was performed. Consistent with the immunohistochemistry results in Figure 2A, the ATF3 expression level was highly upregulated at 7 dpl following administration of 10 μg 6-OHDA, but this upregulation was alleviated in response to 20 μg 6-OHDA (Figure 2C and D). This decline in ATF3 expression level was probably due to the significant loss of DA neurons in the 20 μg 6-OHDA-treated group.

Next, we examined the morphological characteris-

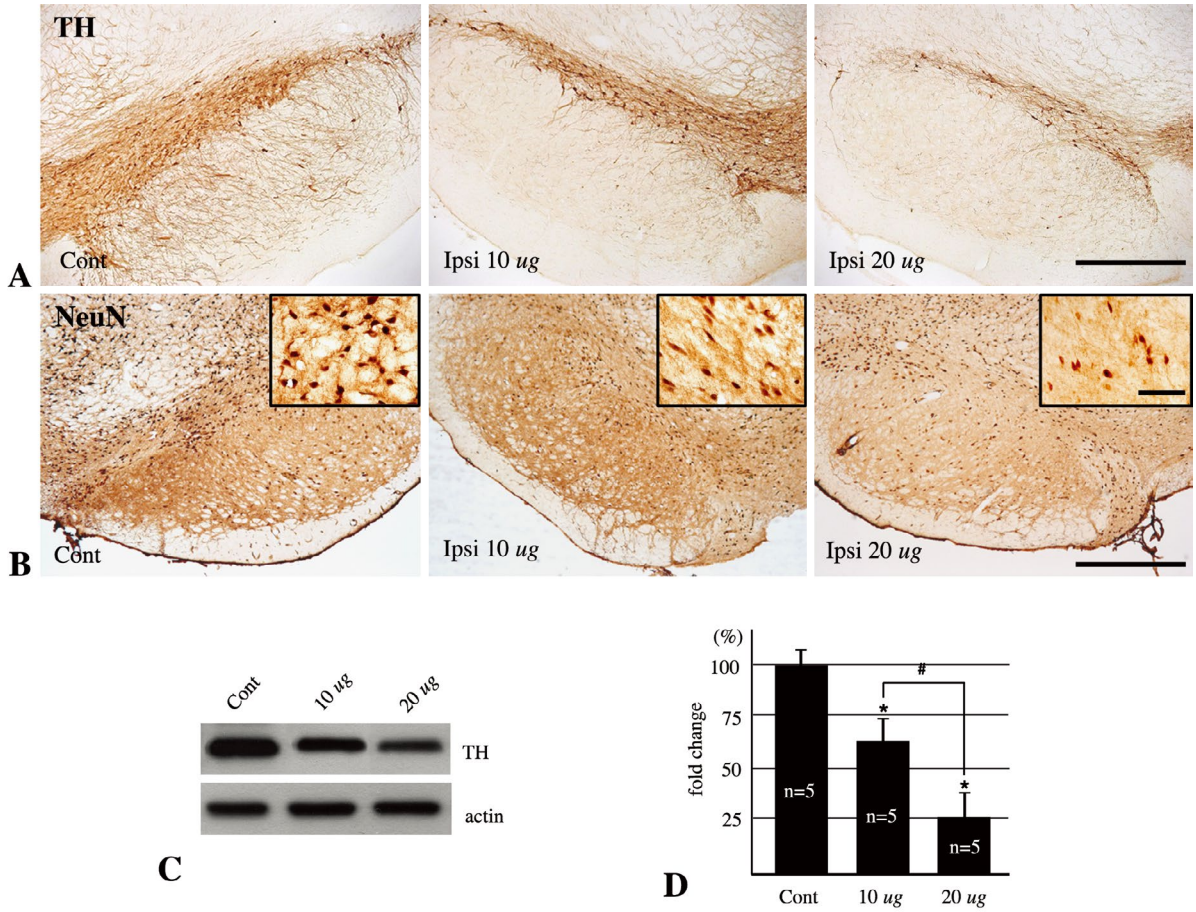

Figure 1. Dose-dependent loss of TH-ir neurons induced by 6-OHDA in the ipsilateral SN. (A) Photographs of TH immunohistochemistry in the contralateral (Cont) and ipsilateral (Ipsi) SN after exposure with 10 or 20 μg 6-OHDA at 7 days post-lesion (dpl). A significant reduction in the number of TH-ir neurons was noted in the ipsilateral SN. (B) NeuN immunohistochemistry. Insets in (B) represent higher magnification of each photograph, particularly the SNpc. Compared with other areas (i.e., red nucleus or SNpr), the number of NeuN-ir neurons in the SNpc decreased markedly in the ipsilateral SN after 6-OHDA treatment. Scale bars in (A) and (B) are 300 μm, and scale bar in inset of (B) is 50 μm. (C) Changes in TH expression levels by Western blot assay. (D) Quantification of results from Western blot assay in (C). TH band density was normalized against that of β-actin. Values are normalized to the control and expressed as mean ± SE (n = 5). $^{*}P < 0.05$ compared with control value and $^{\#}P < 0.05$ compared with value from 10 μg 6-OHDA-treated group (ANOVA with *post-hoc* Student's *t*-test).

tics of degenerating DA neurons by H & E staining to reveal whether the DA neuronal cell death following 6-OHDA exposure was apoptotic or necrotic because ATF3 and cell apoptosis are closely related[18]. In the contralateral SNpc, numerous large DA neurons showed normal morphology with a large cytoplasm, polygonal shape, emanating processes, and slightly stained nuclei with prominent nucleoli (Figure 3A and C). However, in the ipsilateral SNpc, an increased number of degenerating DA neurons with shrunken soma and eosinophilic perikarya were observed (Figure 3B, D, and E). In some specimens, we noted a number of apoptotic cells whose nuclei were condensed and fragmented into small round bodies (Figure 3F-H). These morphological figures suggest that 6-OHDA-induced DA neuronal cell death may be apoptosis. Nevertheless, they did not react to terminal deoxynucleotidyl transferase (TdT)-mediated dUTP nick end labeling (TUNEL) (data not shown).

Nuclear translocation of AIF may play an important role in 6-OHDA-induced toxicity

AIF protein expression was examined in the SNpc using immunohistochemistry and double immunofluorescence 7 dpl after 6-OHDA treatment. AIF immunoreactivity was detected in the cytoplasm and processes at both of SNpc DA neurons (arrows in Figure 4C and D). However, specific AIF immunoreactivity in the nucleus and cytoplasm was only observed in some ipsilateral SNpc

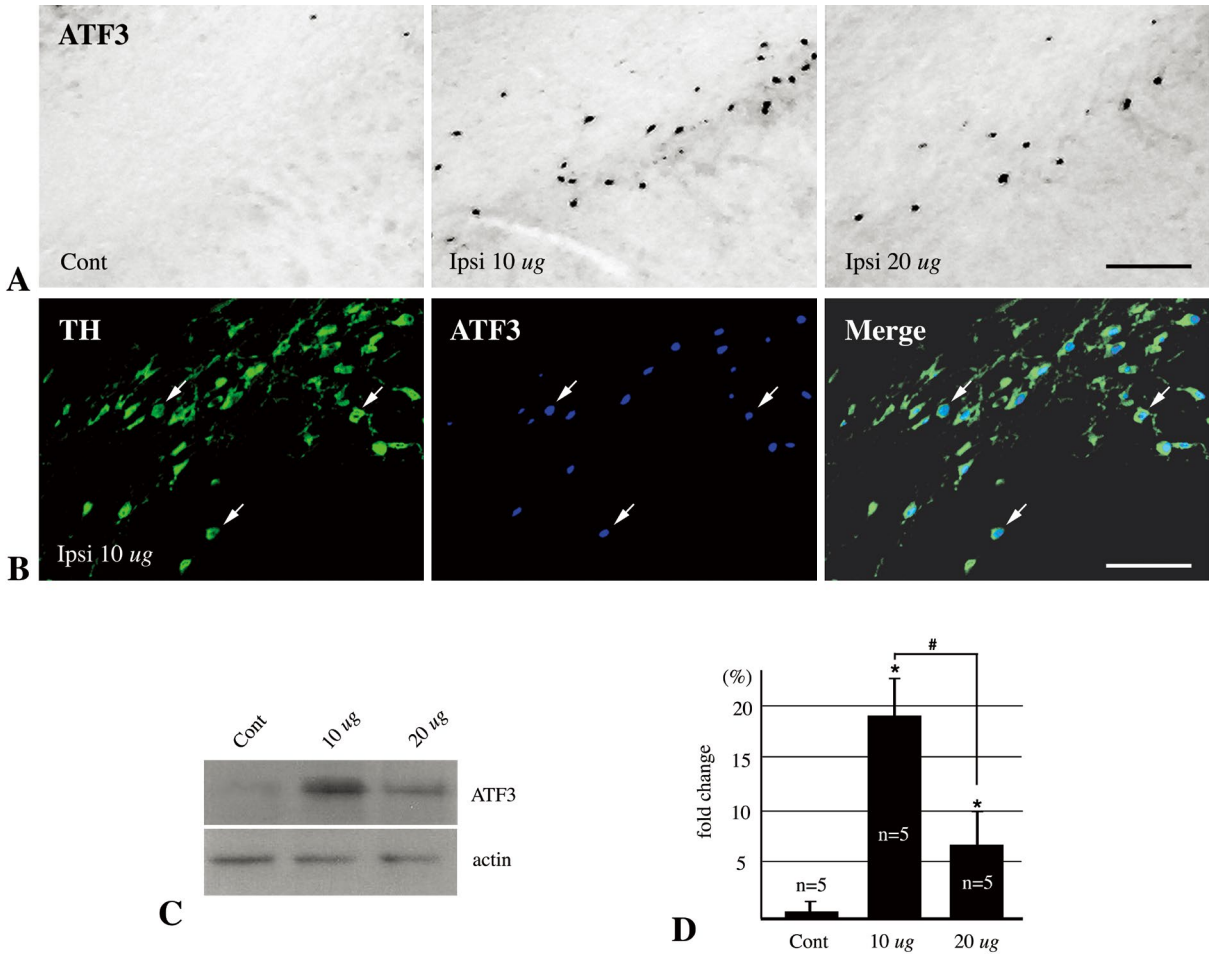

Figure 2. ATF3 expression is upregulated by 6-OHDA treatment in TH-ir neurons. (A) Photographs of ATF3 immunohistochemistry in the contralateral (Cont) and ipsilateral SN after the MFB of animals was treated with 10 or 20 μg 6-OHDA at 7 dpl. Following 6-OHDA treatment, specific ATF3 induction was identified in the ipsilateral SN. (B) Double immunofluorescence images of TH, ATF3, and their merged image. Many TH-ir neurons are co-localized with ATF3 (arrows). Scale bars in (A) and (B) are 100 μm. (C) Changes in ATF3 expression levels by Western blot assay. (D) Quantification of Western blot results. ATF3 band density was normalized against that of β-actin. Values were normalized to the control and expressed as mean ± SE (n = 5). $^{*}P < 0.05$ compared with control value and $^{\#}P < 0.05$ compared with value from 10 μg 6-OHDA-treated group (ANOVA with *post-hoc* Student's *t*-test).

specimens (arrowheads in Figure 4D). To confirm that AIF nuclear localization in the ipsilateral SNpc, double-immunofluorescent labeling of AIF and TH was performed. Nuclei were also visualized with Hoechst 33258. Consistent with the immunohistochemistry results, most of the contralateral and ipsilateral AIF immunofluorescence labeling of TH-ir DA neurons was cytoplasmic (Figure 4E). However, in some specimens of ipsilateral SNpc, nuclear localization of AIF was observed in the 6-OHDA treated DA neurons (Figure 4F). In sections where the AIF primary antibody had been omitted, AIF immunoreactivity was not seen, confirming the specificity of the anti-AIF antibody.

Discussion

In 1968, Ungerstedt showed that 6-OHDA administration into the SNpc induced anterograde degeneration of the nigrostriatal DA system; thus, generating the first PD animal model[2]. Since then, the 6-OHDA animal model has been the most widely used tool for replicating a PD-like loss of DA neurons in the SNpc. 6-OHDA exerts specific neurotoxicity on catecholaminergic neurons by selective uptake through the DA transporter and by generating H_2O_2, superoxide, and cytotoxic hydroxyl radicals, which directly damage cells[19]. Other effects, including direct inhibition of mitochondrial complexes I and IV and alterations in

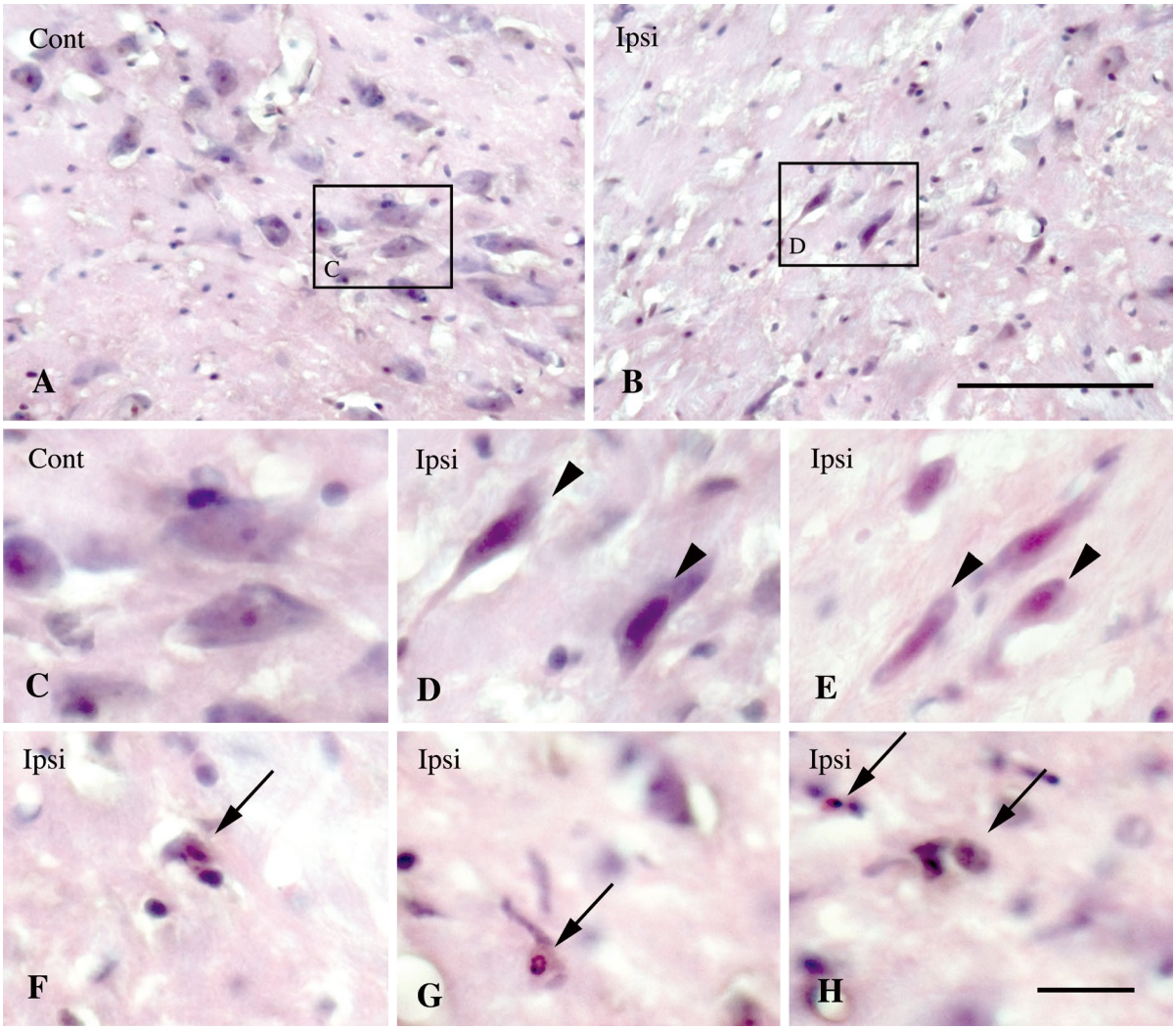

Figure 3. 6-OHDA produces apoptotic DA neuronal cell death in H & E staining. Representative photographs of contralateral (Cont, A and C) and ipsilateral (Ipsi, B, and D-H) SNpc after 10 μg 6-OHDA treatment at 7 dpl. (C) and (D) are high magnification of (A) and (B), respectively. Typical healthy DA neurons are observed in the contralateral SNpc; large cytoplasm, polygonal shape, emanating processes, and slightly stained nuclei with prominent nucleoli (A and C). However, photographs in (E-H) are taken from ipsilateral SNpc from other tissue sections. Many degenerating neurons characterized by shrunken soma with eosinophilic perikarya are noted in the ipsilateral SNpc (arrowheads in D and E). Note the number of apoptotic cells whose nuclei are condensed in typical crescent form or fragmented into small round bodies (arrows in F-H). Scale bars are 100 μm in (A and B) and 25 μm in (C and D), respectively.

cytoplasmic calcium homeostasis have also been described[20]. Dopamine itself has been considered a major risk factor in PD because it is readily oxidized to highly cytotoxic quinone molecules *in vitro* and *in vivo*[6]. Moreover, dopamine can be converted to 6-OHDA in the presence of transition metals and H_2O_2[19]. 6-OHDA and other quinone molecules have been detected in post-mortem Parkinsonian brains[5]. Therefore, understanding the underlying mechanisms of 6-OHDA cytotoxicity in the DA nigrostriatal system could lead to significant improvement in Parkinsonism therapies.

Selective degeneration of DA neurons can be achieved by local administration of 6-OHDA. Several brain regions composing the nigrostriatal system can be used as site to develop a PD animal model, including injecting 6-OHDA directly into the striatum, the SN, or the MFB. The injection is commonly carried out unilaterally, with the contralateral brain serving as an internal control[21,22]. Intra-striatal administration of 6-OHDA usually results in a progressive loss of DA neurons over the course of several weeks. However, this method may fluctuate according to the amount, number, and loca-

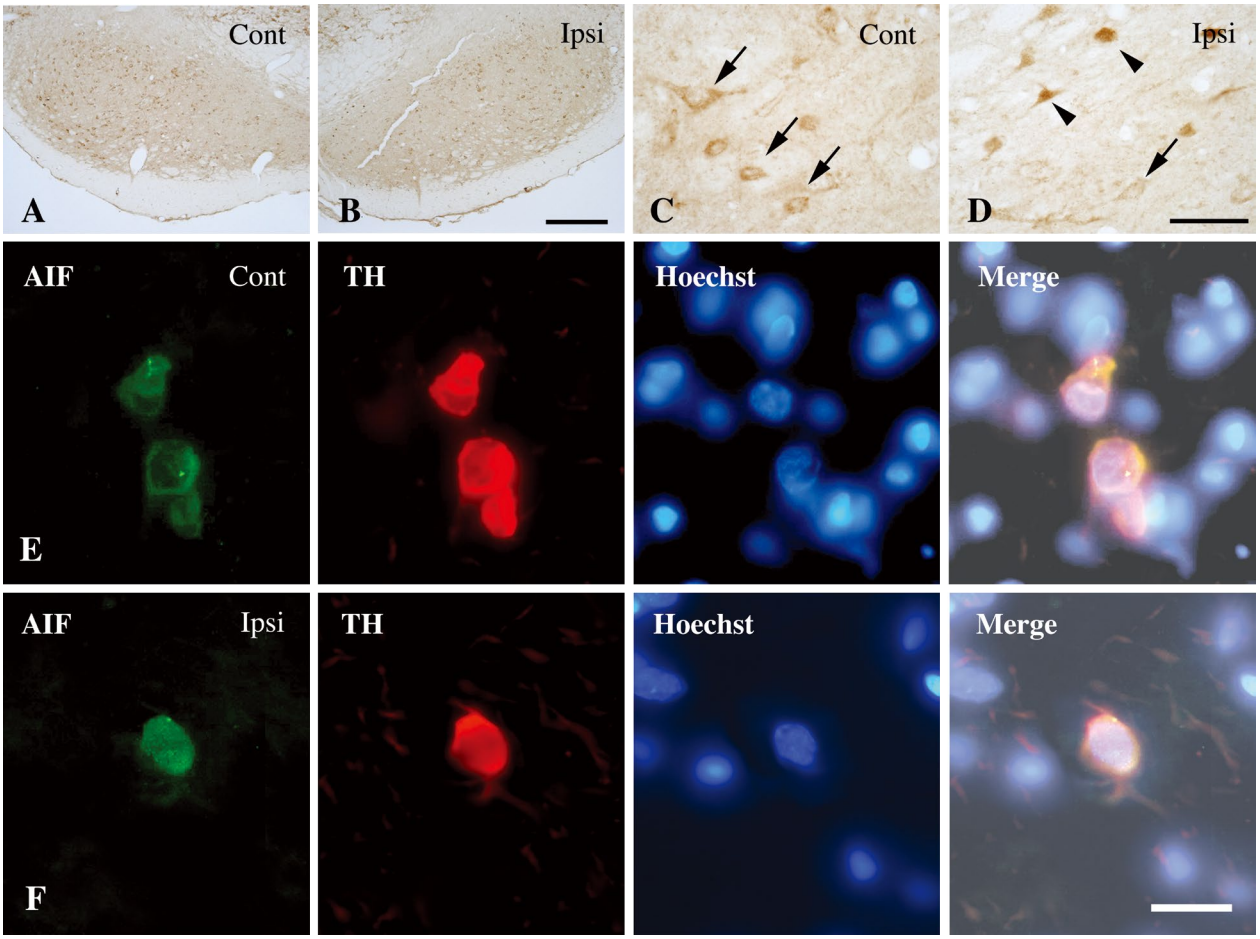

Figure 4. AIF translocation was induced in the ipsilateral TH-ir DA neurons after 6-OHDA treatment. (A-D) Representative photographs of AIF immunohistochemistry in the contralateral (A and C) SNpc and ipsilateral (B and D) SNpc at 7 dpl after 10 μg 6-OHDA treatment. (B) and (D) are high magnification images of (A) and (C). Most all DA neurons in the contralateral and ipsilateral SNpc showed the same AIF immunoreactivity patterns; AIF immunoreactivity was mainly detected in the cytoplasm and processes, but not in the nucleus (arrows in C and D). However, AIF-ir nuclei (arrowheads in D) were detected in some ipsilateral SNpc specimens. (E and F) Double immunofluorescent labeling of AIF and TH in the contralateral (E) and ipsilateral (F) SNpc at 7 days after 6-OHDA treatment. Nuclei were visualized with Hoechst 33258. In accordance with the AIF immunohistochemistry results, most of the contralateral and ipsilateral TH-ir neurons show AIF immunoreactivity in the cytoplasm (E). However, a few DA neurons in ipsilateral SNpc showed AIF immunoreactivity in nuclei (F). Scale bars in (B), (D), and (F) are 500, 50, and 20 μm, respectively.

tion of injections. The remaining two methods usually result in acute loss of DA neurons in the SNpc and relatively consistent results can be obtained. However, the intra-nigral method can cause direct physical damage to DA neurons, so MFB administration was used in this study.

The present study confirmed that 6-OHDA injection into the MFB leads to a massive loss of TH-ir neurons in a dose-dependent manner (Figure 1A and 1C). DA neuronal cell loss was also confirmed by NeuN immunohistochemistry (Figure 1B). It has been generally established that apoptosis or an apoptosis-like cell death pathway contributes to neuronal cell loss in most neurodegenerative disorders. Therefore, ATF3 immunolabeling was employed in our model to test the type of cell death mechanism because ATF3 and cell apoptosis are closely related. In normal cells, ATF3 is generally expressed at low levels, but can be rapidly upregulated in response to diverse stress signals, such as nerve injury or ischemia, and lead to act as transcription factor[23,24]. Although the roles of ATF3 related to cell survival and regeneration have been suggested[25,26], persistent expression of ATF3 primarily induces cell death. We previously demonstrated that transecting the MFB leads to co-localization of ATF3 and phosphorylated c-Jun in degenerating DA neurons, which specif-

ically adhered to activated and phagocytic microglia throughout the entire neurodegenerative processes in the SN[17]. We also reported that middle carotid artery occlusion and reperfusion injury induces activation of ATF3 in the peri-infarct region and that about 15% of ATF3-ir neurons in the ischemic penumbra region express caspase 3[27]. These findings strongly support the putative role of ATF3 as an apoptosis inducer.

The present findings demonstrate that 6-OHDA significantly up-regulated ATF3 expression in DA neurons (Figure 2). The ATF3 expression level in the 10 μg 6-OHDA-treated group was higher than that in the 20 μg 6-OHDA-treated group. This decrease was probably due to the significant loss of DA neurons in the 20 μg 6-OHDA-treated group. Next, we performed a TUNEL analysis to confirm that the DA neuronal cell death in response to 6-OHDA was caused by apoptosis but no TUNEL-positive results were observed. However, these results do not exclude the possibility that 6-OHDA-induced DA neuronal cell death is apoptosis or apoptosis-like cell death because our H & E results showed many degenerating neurons with typical morphological characteristics of apoptosis, such as shrunken soma, eosinophilic perikarya, and condensed or fragmented nuclei (Figure 3).

Although TUNEL analysis has rapidly become the most widely used *in situ* test for detecting apoptosis, it has been critically reviewed because it and currently used related methods do not always distinguish between apoptosis and necrosis[28,29]. Therefore, the failure to demonstrate apoptosis by traditional apoptotic criteria, such as a TUNEL analysis, in a particular pathological condition does not preclude the involvement of an apoptosis or the apoptosis-like cell death pathway. Thus, the present results suggest that the DA neuronal cell death induced by 6-OHDA was another type of apoptosis, such as apoptosis-like caspase-independent apoptosis[30].

AIF has been proposed to act as a putative ROS scavenger in the mitochondrial intermembrane space[12]. For example, AIF-depleted *Harlequin* mice, which exhibit a 40-50% deficiency in brain mitochondrial complex I, do not display any deficits in the nigrostriatal DA pathway, although they showed cerebellar and retinal degeneration[31]. However, the nigrostriatal system of these animals is much more susceptible to exogenous neurotoxins, such as MPTP and rotenone[31,32]. These results suggest that AIF plays an antioxidant role. Meanwhile, upon pathological permeabilization of the outer mitochondrial membrane, AIF (mitochondrial-confined 67 kDa isoform) is processed to a soluble 57 kDa form which is readily available for translocation. Cleavage seems to be achieved through activation of cysteine proteases different from caspases, such as cathepsins and/or calpains[13]. The soluble proapoptotic isoform of AIF is now called tAIF. tAIF is released from mitochondria and translocated to the nucleus via its C-terminal nuclear localization sequence, leading to large-scale DNA fragmentation of approximately 50 kbp, which is a hallmark of caspase-independent apoptosis[13,15].

Programmed cell death (PCD) is believed to contribute to neuronal cell loss in various neurodegenerative diseases, such as Alzheimer disease (AD), PD, and multiple sclerosis[33,34]. Various caspase-dependent cascades are important mediators of neuronal PCD in neurodegenerative diseases[35]. However, accumulating evidences also suggest that AIF-induced, caspase-independent neuronal PCD can be involved in the progression of neurodegenerative diseases. Yu and colleagues promoted this hypothesis by showing that neuronal AIF, which is intimately linked to neurofibrillary tangles (primary marker of AD), is upregulated in the AD limbic cortex, and that nuclear localization of AIF increased[36]. Burguillos *et al*. also observed nuclear translocation of AIF in the ventral mesencephalon in a PD postmortem study[37].

Recently, evidences for the involvement of AIF in 6-OHDA-induced DA neuronal cell death have been suggested in both *in vivo* and *in vitro* PD models[38,39]. In this study, authors have detected the morphological features of PCD in degenerating DA neurons and specific induction of ATF3, but the TUNEL negative data suggested the possibility that DA neuronal loss caused by 6-OHDA neurotoxicity may be caspase-independent, AIF-induced apoptosis. To test this possibility, we performed immunohistochemistry and immunofluorescence analyses using anti-AIF antisera in our models. Consistent with other reports[38,40], AIF immunopositive signals were diffusely distributed in the cytosol in most all large neurons in the contralateral and ipsilateral SN, whereas confined nuclear localization of AIF immunoreactivity could be observed in the ipsilateral SN (Figure 4).

In conclusion, we have provided additional *in vivo* evidence supporting a role for AIF-dependent DA neuronal apoptosis in an experimental PD animal model. We also presented the possible role of ATF3 in AIF-induced apoptosis. However, this does not rule out the possibility of other cell death cascades, such as caspase-dependent apoptosis. Further studies will be required to define the precise mechanisms through which AIF act to trigger 6-OHDA neurotoxicity to DA neurons.

Materials & Methods

Animal care

All experimental procedures were carried out accord-

ing to the National Institutes of Health Guide for the Care and Use of Laboratory Animals (NIH Publication No. 80-23, revised 1996) under approval of the Eulji University Institutional Animal Care and Use Committee. All efforts were made to minimize the numbers of animals used and ensure minimal suffering of those animals. Adult male Sprague-Dawley rats (body weight, 250-300 g; Charles River Lab, Wilmington, DE, USA) were used. The animals were housed with food and water freely available in a room maintained at constant room temperature (20-22°C) and a 12 : 12-h light-dark cycle.

Surgical procedures

The rats were anesthetized with ketamine (70 mg/kg body weight) and xylazine (8 mg/kg body weight) intraperitoneally and secured in a stereotaxic apparatus (Stoelting Co., Wood Dale, IL, USA). The skull was exposed by a midline incision and the periosteum was cleared from the cranium. A small hole was made with a dental drill in the right side of the skull 3.8 mm posterior to the bregma and 1.5 mm lateral to the midline. A 26 gauge steel needle attached to a 10-μL Hamilton syringe (Hamilton Co., Reno, NV, USA) was lowered through the hole to a depth of 8.0 mm from the skull. Either 10 or 20 μg 6-OHDA (Sigma-Aldrich, St. Louis, MO, USA) dissolved in 4 μL of 0.02 mg/mL ascorbate-saline was administered. The injection was made using a micro-infusion pump (KD Scientific Inc., Holliston, MA, USA), at a rate of 0.5 μL/min. The needle was left in place for a further 5 min before slowly retracting it from the brain, and the skin was sutured. After surgery, the animals were kept on a heating pad at 37°C until recovery was complete. Six to seven rats were killed at various time points from 1 day to 4 weeks post-lesion. The left sides of the brains were used as internal controls.

Sample preparation

The experimental animals were re-anesthetized as described above and perfused through the ascending aorta with 200 mL 4% paraformaldehyde in 0.1 M phosphate buffered saline (PBS) for immunohistochemistry and immunofluorescence. The brains were removed carefully and placed on a Rat Brain Blocker (David Kopf Instruments, Tujunga, CA, USA) and then sliced into 10-mm-coronal blocks that included the SN, according to the atlas of Paxinos and Watson[41]. The sliced brain blocks were post-fixed for 2 h in the same fixative and infiltrated with 30% sucrose solution for 12 h at 4°C until they sank. The sliced blocks were frozen rapidly in 2-methylbutane chilled on dry ice and mounted in Tissue-Tek OCT compound (Sakura Finetechnical Co., Tokyo, Japan). Serial coronal sections of 40-μm-thickness were obtained on a Cryostat Microtome (Leica Microsystems Inc., Wetzlar, Germany). Every twelfth section was collected at a periodicity of 480 μm as one set, so 12 sets were prepared for each sliced brain block. To observe the morphological integrity and characteristics following administration of 6-OHDA, one set of sections was stained with hematoxylin and eosin (H & E).

Immunohistochemistry

The sections were washed for 10 min in 0.1 M PBS and endogenous peroxidase activity was quenched by incubating the tissue sections with 0.3% hydrogen peroxide in PBS for 30 min. The sections were rinsed in PBS and incubated in PBS containing 10% normal serum from the same host species as the secondary antibody and 0.1% Triton X-100 for 1 h to reduce non-specific staining. The sections were incubated with primary antibodies, diluted in 0.1 M PBS containing 0.1% Triton X-100 (PBST) at 4°C overnight. The primary antibodies were as follows: mouse monoclonal anti-neuronal nuclei (NeuN) antibody (1 : 500; Chemicon, Temecula, CA, USA), mouse monoclonal anti-tyrosine hydroxylase (TH) antibody (1 : 1,000; Chemicon), rabbit polyclonal anti-activating transcription factor 3 (ATF3) and goat polyclonal anti-AIF antibody (1 : 500; Santa Cruz Biotechnology, Delaware, CA, USA). These primary antibodies are summarized in Table 1. The sections were washed three times with PBST and incubated for

Table 1. Overview of the primary antibodies used in this study

Antibodies	Company	Purpose of use	Dilution
NeuN	Chemicon	used to identify and differentiate the neurons from neuroglia in CNS parenchyma[27]	1 : 500 for IHC
TH	Chemicon	used to examine the DA neurons in the rat SNpc[7-10]	1 : 1,000 for IHC 1 : 100 for IF
ATF3	Santa Cruz	used to detect the 6-OHDA insulted DA neurons undergoing gradual apoptotic degeneration[17]	1 : 500 for IHC 1 : 50 for IF
AIF	Santa Cruz	used to identify the AIF expressing neurons and its cellular localization[11,13]	1 : 500 for IHC 1 : 100 for IF

2 h with biotinylated goat anti-mouse immunoglobulin G (IgG) (1 : 200; Vector Labs, Burlingame, CA, USA) for NeuN and TH, with biotinylated horse anti-rabbit IgG (1 : 200; Vector Labs) for ATF3 or with biotinylated horse anti-goat IgG (1 : 200; Vector Labs) for AIF, followed by incubation for 1 h with Avidin-Biotin Peroxidase Complex. Antigens were visualized with 3,3′-diaminobenzidine tetrahydrochloride (DAB; Sigma-Aldrich) solution containing 0.003% hydrogen peroxide. Sections were mounted on gelatin-coated slides, dehydrated through a graded ethanol series, cleared in xylene, and coverslipped with Permount. The specificity of the immunolabeling was validated by omitting the primary antibodies.

Double immunofluorescence labeling

Double-immunofluorescence labeling of ATF3/TH and AIF/TH was conducted to examine which cell type expresses ATF3 or AIF in SN and their subcellular localization. Following incubation in PBST containing 10% normal horse serum for 1 h, the sections were incubated overnight at 4°C with TH antibody diluted 1 : 100 in PBST. After rinsing in PBST, a FITC-conjugated horse anti-mouse secondary antibody for ATF3/TH and a Cy3-conjugated horse anti-mouse secondary antibody for AIF/TH were applied for 2 h at room temperature. After a brief rinse, the ATF3 (1 : 50) and AIF antibody (1 : 100) was applied for 36 h at 4°C, followed by an AMCA-conjugated horse anti-rabbit secondary antibody for ATF3/TH and a FITC-conjugated horse anti-goat secondary antibody for AIF/TH application for 2 h. All secondary antibodies were purchased from Jackson Labs (Jackson ImmunoResearch Labs., West Grove, PA, USA) and 1 : 150 dilutions were used. For AIF/TH double labeling, sections were incubated with Hoechst 33342 (Sigma-Aldrich) to visualize the nuclei.

Digital photography

Light and fluorescent micrographic images were acquired on an Olympus Ax 70 microscope (Olympus Inc., Tokyo, Japan) fitted with a Carl Zeiss AxioCam MRC digital camera (Carl Zeiss Inc., Jena, Germany), using AxioVision ver. 4.6 image capture software (Carl Zeiss). These images were imported into the Adobe Photoshop ver. 6.0 (Adobe Systems Inc., San Jose, CA, USA) and adjusted for brightness and contrast to optimized photographic presentation of images. The fluorescent images were merged and presented using the Adobe Photoshop program.

Western blot analysis

Following cardiac perfusion with normal saline, about 5 mm coronal brain block including SN was obtained. The tissue block was cut through the arbitrary horizontal line crossing the inferior border of the both medial geniculate bodies, and then cut through the arbitrary vertical line dividing SN into right and left haves. The isolated tissue block were homogenized in a protein extraction solution (Pro-prep protein extraction solution; Intron Biotech, Seoul, Korea) using a Polytron homogenizer (Fisher Scientific, Pittsburgh, PA, USA). Protein content was measured using a Bio-Rad colorimetric protein assay kit (Bio-Rad, Hercules, CA, USA). A 20 mg protein sample was separated by sodium dodecyl sulfate-polyacrylamide gel electrophoresis and transferred onto a nitrocellulose membrane (Invitrogen, Carlsbad, CA, USA). The mouse monoclonal anti-β-actin (1 : 5,000, Chemicon), TH (1 : 2,000) and ATF3 (1 : 1,000) antibodies were used as primary antibodies and horseradish peroxidase-conjugated antibody (1 : 500; Amersham Pharmacia Biotech, Woodlawn, IL, USA) was used as a secondary antibody. Bands were detected using the enhanced chemiluminescence detection system (Amersham Pharmacia Biotech). Quantification was performed using Image J software. The density of each TH and ATF3 band was normalized against that of β-actin.

Acknowledgements This work was partly supported by Institute for Information & communications Technology Promotion (IITP) grant funded by the Korea government (MSIP) (No. B0132151001000303, Next Imaging System XIS) and partly supported by Basic Science Research Program through the National Research Foundation of Korea (NRF) funded by the Ministry of Education, Science and Technology (NRF-2015R1D1A3A03020164).

Conflict of Interest Hong-Il Yoo declares that he has no conflict of interest. Gil-Yeong Ahn declares that he has no conflict of interest. Eun-Jin Lee declares that she has no conflict of interest. Eu-gene Kim declares that she has no conflict of interest. Sung-Young Hong declares that he has no conflict of interest. Sang-Jin Park declares that he has no conflict of interest. Ran-Sook Woo declares that she has no conflict of interest. Tai-Kyoung Baik declares that he has no conflict of interest. Dae-Yong Song declares that he has no conflict of interest.

Human and animal rights All animal studies were approved by the Animal Care Committee of Eulji University, and all husbandry practices and animal care were in accordance with the guidelines of Korean Council on Animal Care.

References

1. Fahn, S. & Cohen, G. The oxidant stress hypothesis in

Parkinson's disease: evidence supporting it. *Ann Neurol* **32**:804-812 (1992).
2. Ungerstedt, U. 6-Hydroxy-dopamine induced degeneration of central monoamine neurons. *Eur J Pharmacol* **5**:107-110 (1968).
3. Davis, G. C. *et al*. Chronic Parkinsonism secondary to intravenous injection of meperidine analogues. *Psychiatry Res* **1**:249-254 (1979).
4. Curtius, H. C., Wolfensberger, M., Steinmann, B., Redweik, U. & Siegfried, J. Mass fragmentography of dopamine and 6-hydroxydopamine. Application to the determination of dopamine in human brain biopsies from the caudate nucleus. *J Chromatogr* **99**:529-540 (1974).
5. Spencer, J. P. *et al*. Conjugates of catecholamines with cysteine and GSH in Parkinson's disease: possible mechanisms of formation involving reactive oxygen species. *J Neurochem* **71**:2112-2122 (1998).
6. Stokes, A. H., Hastings, T. G. & Vrana, K. E. Cytotoxic and genotoxic potential of dopamine. *J Neurosci Res* **55**:659-665 (1999).
7. Choi, W. S. *et al*. Two distinct mechanisms are involved in 6-hydroxydopamine- and MPP^+-induced dopaminergic neuronal cell death: role of caspases, ROS and JNK. *J Neurosci Res* **57**:86-94 (1999).
8. von Coelln, R. *et al*. Rescue from death but not from functional impairment: caspase inhibition protects dopaminergic cells against 6-hydroxydopamine-induced apoptosis but not against the loss of their terminals. *J Neurochem* **77**:263-273 (2001).
9. O'Malley, K. L., Liu, J., Lotharius, J. & Holtz, W. Targeted expression of BCL-2 attenuates MPP^+ but not 6-OHDA induced cell death in dopaminergic neurons. *Neurobiol Dis* **14**:43-51 (2003).
10. Ebert, A. D., Hann, H. J. & Bohn, M. C. Progressive degeneration of dopamine neurons in 6-hydroxydopamine rat model of Parkinson's disease does not involve activation of caspase-9 and caspase-3. *J Neurosci Res* **86**:317-325 (2008).
11. Daugas, E. *et al*. Mitochondrio-nuclear translocation of AIF in apoptosis and necrosis. *FASEB J* **14**:729-739 (2000).
12. Klein, J. A. *et al*. The harlequin mouse mutation downregulates apoptosis-inducing factor. *Nature* **26**:367-374 (2002).
13. Otera, H., Ohsakaya, S., Nagaura, Z., Ishihara, N. & Mihara, K. Export of mitochondrial AIF in response to proapoptotic stimuli depends on processing at the intermembrane space. *EMBO J* **24**:1375-1386 (2005).
14. Lorenzo, H. K., Susin, S. A., Penninger, J. & Kroemer, G. Apoptosis inducing factor (AIF): a phylogenetically old, caspase-independent effector of cell death. *Cell Death Differ* **6**:516-524 (1999).
15. Susin, S. A. *et al*. Molecular characterization of mitochondrial apoptosis-inducing factor. *Nature* **397**:441-446 (1999).
16. Susin, S. A. *et al*. Two distinct pathways leading to nuclear apoptosis. *J Exp Med* **192**:571-580 (2000).
17. Song, D. Y. *et al*. Axotomy-induced dopaminergic neurodegeneration is accompanied with c-Jun phosphorylation and activation transcription factor 3 expression. *Exp Neurol* **209**:268-278 (2008).
18. Pu, H. *et al*. Heroin activates ATF3 and CytC via c-Jun N-terminal kinase pathways to mediate neuronal apoptosis. *Med Sci Monit Basic Res* **21**:53-62 (2015).
19. Blum, D. *et al*. Molecular pathways involved in the neurotoxicity of 6-OHDA, dopamine and MPTP: contribution to the apoptotic theory in Parkinson's disease. *Prog Neurobiol* **65**:135-172 (2001).
20. Glinka, Y. & Youdim, M. B. Inhibition of mitochondrial complexes I and IV by 6-hydroxydopamine. *Eur J Pharmacol* **292**:329-332 (1995).
21. Sauer, H. & Oertel, W. H. Progressive degeneration of nigrostriatal dopamine neurons following intrastriatal terminal lesions with 6-hydroxydopamine: a combined retrograde tracing and immunocytochemical study in the rat. *Neuroscience* **59**:401-415 (1994).
22. Lee, C. S., Sauer, H. & Bjorklund, A. Dopaminergic neuronal degeneration and motor impairments following axon terminal lesion by instrastriatal 6-hydroxydopamine in the rat. *Neuroscience* **72**:641-653 (1996).
23. Dragunow, M. *et al*. Is c-Jun involved in nerve cell death following status epilepticus and hypoxic-ischaemic brain injury? *Brain Res Mol Brain Res* **18**:347-352 (1993).
24. Kawauchi, J. *et al*. Transcriptional repressor activating transcription factor 3 protects human umbilical vein endothelial cells from tumor necrosis factor-alpha-induced apoptosis through down-regulation of p53 transcription. *J Biol Chem* **277**:39025-39034 (2002).
25. Nakagomi, S., Suzuki, Y., Namikawa, K., Kiryu-Seo, S. & Kiyama, H. Expression of the activating transcription factor 3 prevents c-Jun N-terminal kinase-induced neuronal death by promoting heat shock protein 27 expression and Akt activation. *J Neurosci* **23**:5187-5196 (2003).
26. Park, S. H. *et al*. Activating transcription factor 3-mediated chemo-intervention with cancer chemokines in a noncanonical pathway under endoplasmic reticulum stress. *J Biol Chem* **289**:27118-27133 (2014).
27. Song, D. Y. *et al*. Role of activating transcription factor 3 in ischemic penumbra region following transient middle cerebral artery occlusion and reperfusion injury. *Neurosci Res* **70**:428-434 (2011).
28. Stadelmann, C. & Lassmann, H. Detection of apoptosis in tissue sections. *Cell Tissue Res* **301**:19-31 (2000).
29. Huerta, S., Goulet, E. J., Huerta-Yepez, S. & Livingston, E. H. Screening and detection of apoptosis. *J Surg Res* **139**:143-156 (2007).
30. Krantic, S., Mechawar, N., Reix, S. & Quirion, R. Apoptosis-inducing factor: a matter of neuron life and death. *Prog Neurobiol* **81**:179-196 (2007).
31. Perier, C. *et al*. Apoptosis-inducing factor deficiency sensitizes dopaminergic neurons to parkinsonian neurotoxins. *Ann Neurol* **68**:184-192 (2010).
32. Choi, W. S., Kruse, S. E., Palmiter, R. D. & Xia, Z. Mitochondrial complex I inhibition is not required for

dopaminergic neuron death induced by rotenone, MPP^+, or paraquat. *Proc Natl Acad Sci* **105**:15136-15141 (2008).
33. Jason, R., Cannon, J. & Timothy, G. The Role of Environmental Exposures in Neurodegeneration and Neurodegenerative Diseases. *Toxicol Sci* **124**:225-250 (2011).
34. Matthew, D. L., Terry, C. B., Alexander, A. M. & Purvesh, K. Integrated multi-cohort transcriptional meta-analysis of neurodegenerative diseases. *Acta Neuropathol Commun* **2**:93 (2014).
35. LeBlanc, A. C. The role of apoptotic pathways in Alzheimer's disease neurodegeneration and cell death. *Curr Alzheimer Res* **2**:389-402 (2005).
36. Yu, W., Mechawar, N., Krantic, S. & Quirion, R. Evidence for the Involvement of Apoptosis-Inducing Factor-Mediated Caspase-Independent Neuronal Death in Alzheimer Disease. *Am J Pathol* **176**:2209-2218 (2010).
37. Burguillos, M. A. *et al*. Apoptosis-inducing factor mediates dopaminergic cell death in response to LPS-induced inflammatory stimulus: evidence in Parkinson's disease patients. *Neurobiol Dis* **41**:177-188 (2011).
38. Kim, T. W. *et al*. Dissociation of progressive dopaminergic neuronal death and behavioral impairments by Bax deletion in a mouse model of Parkinson's diseases. *PLoS One* **6**:e25346 (2011).
39. Ma, C. *et al*. Pre-administration of BAX-inhibiting peptides decrease the loss of the nigral dopaminergic neurons in rats. *Life Sci* **144**:113-120 (2016).
40. Piao, C. S. *et al*. Combined inhibition of cell death induced by apoptosis inducing factor and caspases provides additive neuroprotection in experimental traumatic brain injury. *Neurobiol Dis* **46**:745-758 (2012).
41. Paxinos, G. & Watson, C. The rat brain in stereotaxic coordinates. Academic Press, San Diego (1998).